HYDROLOGICAL PROCESSES
Hydrol. Process. **19**, 2591–2608 (2005)
Published online 19 April 2005 in Wiley InterScience (www.interscience.wiley.com). DOI: 10.1002/hyp.5733

Thermal regime of a headwater stream within a clear-cut, coastal British Columbia, Canada

R. D. Moore,[1,2]* P. Sutherland,[3] T. Gomi[1†] and A. Dhakal[2††]

[1] *Department of Geography, The University of British Columbia, 1984 West Mall, Vancouver, B.C., Canada V6T 1Z2*
[2] *Department of Forest Resources Management, The University of British Columbia, 2424 Main Mall, Vancouver, B.C., Canada V6T 1Z4*
[3] *28 Lansdowne Gardens, Pointe Claire, Quebec, Canada H9S 5B9*

Abstract:

This study examined the thermal regime of a headwater stream within a clear-cut. The stream had a complex morphology dominated by step–pool features, many formed by sediment accumulation upstream of woody debris. Maximum daily temperatures increased up to 5 °C after logging, and were positively associated with maximum daily air temperature and negatively with discharge. Maximum daily temperatures generally increased with downstream distance through the cut block, but decreased with distance in two segments over distances of tens of metres, where the topography indicated relatively concentrated lateral inflow. Localized cool areas within a step–pool unit were associated with zones of concentrated upwelling. Bed temperatures tended to be higher and have greater ranges in areas of downwelling flow into the bed. Heat budget estimates were made using meteorological measurements over the water surface and a model of net radiation using canopy characteristics derived from fisheye photography. Heat exchange driven by hyporheic flow through the channel step was a cooling effect during daytime, with a magnitude up to approximately 25% that of net radiation during the period of maximum daytime warming. Heat budget calculations in these headwater streams are complicated by the heterogeneity of incident solar radiation and channel geometry, as well as uncertainty in estimating heat and water exchanges between the stream and the subsurface via hyporheic exchange and heat conduction. Copyright © 2005 John Wiley & Sons, Ltd.

KEY WORDS stream temperature; forest harvesting; bed temperatures; heat budget; hyporheic exchange

INTRODUCTION

Removal of riparian vegetation cover around small streams can increase incident solar radiation and produce elevated summer stream temperatures, even in some cases where a riparian buffer is retained (e.g., Brown and Krygier, 1970; Hewlett and Fortson, 1982; Johnson and Jones, 2000; Macdonald *et al*., 2003). The ecological effects of logging-related stream temperature changes have been of concern for decades, particularly in relation to temperature-sensitive species such as salmonids (Titcomb, 1926; Beschta *et al*., 1987). Most previous studies of stream temperature response to removal of riparian vegetation focused on the effect at a single measurement location, usually the downstream end of the cut block, and did not consider the potential for thermal heterogeneity at varying spatial scales. Studies in larger stream systems (e.g., third-order) have revealed significant thermal heterogeneity within stream reaches, particularly as a result of local surface–subsurface hydrologic interactions (Malard *et al*., 2001). This heterogeneity can be important in relation to the availability of cool-water areas, which can serve as thermal refugia for temperature-sensitive species such as salmonids during warm periods (Bilby, 1984; Ebersole *et al*., 2003). It also has implications for the representativeness

* Correspondence to: R. D. Moore, Departments of Geography and Forest Resources Management, University of British Columbia, 1984 West Mall, Vancouver, B.C., Canada V6T 1Z2. E-mail: rdmoore@geog.ubc.ca
† Present address: Geo-Hazard Division, Slope Conservation Section, Disaster Prevention Research Institute, Kyoto University, Gokasho, Uji, Kyoto, 611-0011, Japan.
†† Present address: Scotia Pacific Company LLC, Arcata, CA, USA.

Received 23 January 2004
Accepted 16 July 2004

of monitoring locations. However, no studies appear to have examined thermal heterogeneity in smaller, headwater streams.

Bed temperatures can influence the growth and development of benthic invertebrates and fish embryos (Shepherd *et al*., 1986; Malcolm *et al*., 2002), and thus are ecologically significant, but have received less attention than stream temperature. Ringler and Hall (1975) found substantial bed temperature gradients and diurnal variability in a small stream within a clear-cut in Oregon, compared to conditions in a stream draining an unlogged catchment and another that had been 25% patch cut with a riparian buffer. There was significant spatial variability in bed temperature patterns, which Ringler and Hall attributed to the effects of water exchange across the stream bed. Most previous studies of bed temperature patterns, including Ringler and Hall, focused on streams with a riffle–pool morphology. However, many steep headwater streams exhibit a step–pool morphology, which can be associated with significant hyporheic exchange flow, with downwelling into the sediments upstream of the step and upwelling into the downstream pool (Kasahara and Wondzell, 2003). No studies appear to have documented bed temperature patterns associated with a step–pool morphology.

Although the energy budget approach is widely recognized as being the most physically rigorous method for modelling the impacts of forest harvesting on stream temperature, only one study appears to have estimated energy budget components within a clear-cut using microclimatic measurements made over the stream (Brown, 1969). However, that study did not consider the potential effect of hyporheic exchange on the stream heat budget. There is a growing body of evidence that steep headwater channels can experience high rates of hyporheic exchange, and Story *et al*. (2003) estimated that hyporheic exchange was an important contributor to downstream cooling in a headwater stream that had flowed out of forest clearings and back into a full forest canopy environment.

The objectives of this study were: (1) to examine thermal heterogeneity at different spatial scales within a headwater stream reach within a clear-cut; (2) to document bed temperature variations within a step–pool unit and to relate these to surface–subsurface hydrologic interactions; and (3) to estimate the influence of hyporheic exchange through a step–pool unit on the stream heat budget.

METHODS

Study site

The study was conducted in the University of British Columbia Malcolm Knapp Research Forest as part of an interdisciplinary experiment on the effects of varying buffer width on stream–riparian ecology (Kiffney *et al*., 2000). The study area is located approximately 60 km east of Vancouver, B.C., and has a maritime climate with wet, mild winters and warm, dry summers. Mean annual precipitation varies from about 2000 to 2500 mm, of which about 70% falls between October and April as a result of Pacific frontal systems. Because of the maritime climate and low elevation, only about 15% of total annual precipitation falls as snow. Soils are highly permeable, shallow podzols (about 1 m deep) formed in glacial till, underlain by relatively impermeable compacted basal till or granitic bedrock (Hutchinson and Moore, 2000). The forest cover is dominated by western hemlock (*Tsuga heterophylla*) with some western red cedar (*Thuja plicata*) and Douglas fir (*Pseudo-tsuga menziesii*). Prior to the experimental logging, the stands were dominantly mature second growth about 30 to 40 m tall, with crown closure from 75% to 95%.

This study focused on experimental stream A, which was located within a clear-cut with no riparian buffer (Figure 1). Harvesting occurred in 1998. The study reach is 325 m long, and has a mean gradient of 12% and a mean bankfull width of ~4 m. Elevation ranges from 160 to 110 m a.s.l. (Figure 2). Drainage areas at the upstream and downstream ends of the cut block are approximately 46 ha and 59 ha, respectively. Stream morphology is dominated by step–pool structures formed by sediment accumulation upstream of woody debris and boulders, with scour downstream of the steps. The stream flows over bedrock at some locations. The mean pool spacing is about 8 m (Winfield, 2002). The stream provides habitat for both juvenile Coho Salmon (*Oncorhynchus kisutch*) and cutthroat trout (*Oncorhynchus clarki*).

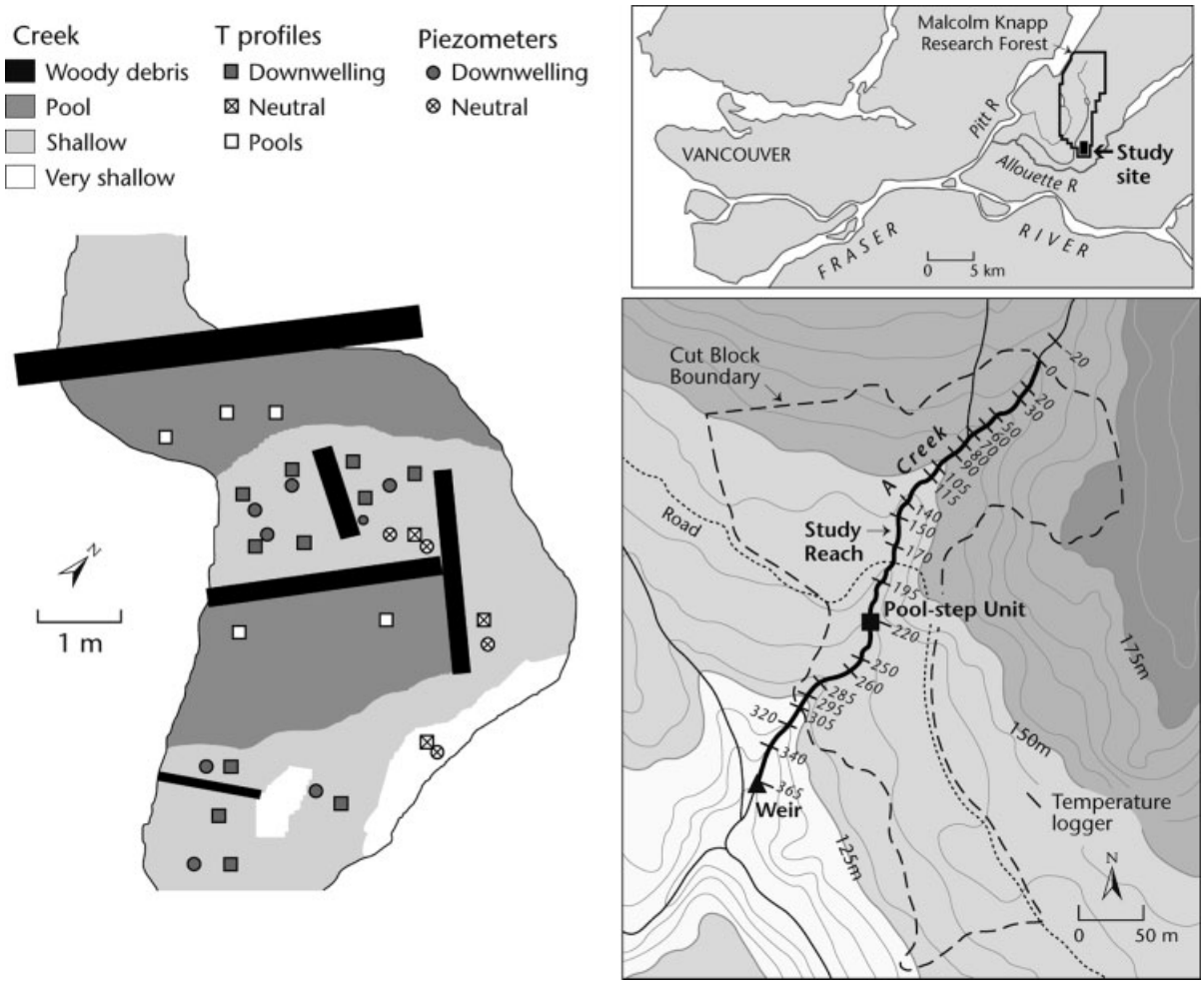

Figure 1. Study site. Right: A Creek showing cut block boundary. Left: step–pool unit with locations of piezometers and thermocouples monitored during 2001

The study also draws upon water temperature data from East Creek, one of the unlogged control streams. East Creek is located about 3 km northwest of A Creek, and at the monitoring site has an elevation of 290 m and a drainage area of 38 ha.

Field measurements

Daily climate measurements are recorded at the Research Forest Headquarters station, located approximately 2 km from A Creek at an elevation of 145 m a.s.l. Measurements include daily maximum and minimum temperature, as well as daily precipitation. Stream temperature was measured using submersible temperature loggers at 13 streams as part of the buffer width experiment. Loggers in the treatment streams were located at the downstream ends of the cut blocks.

In summer 2001, measurements at A Creek focused on conditions throughout the reach within the clear-cut, as well as at a single step–pool unit formed by sediment accumulation upstream of woody debris (Figure 1). Stream water temperature was recorded every 10 min at 24 locations along the study reach using Tidbit submersible temperature loggers, which are accurate to within $\pm 0{\cdot}2\,^{\circ}\mathrm{C}$. To minimize the potential for heating

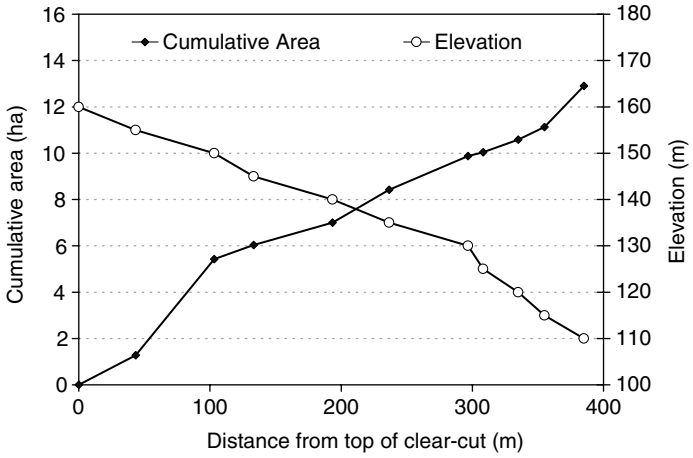

Figure 2. Profiles of elevation and accumulated drainage area along the study reach

by solar radiation absorption, the loggers were housed in 20-cm lengths of 5-cm diameter white PVC pipe with multiple holes drilled through to promote water exchange. Hemispherical photographs were taken at each Tidbit location to determine canopy cover for radiation modelling. In addition, channel cross-sections were measured approximately every 15 m along the stream several times through the study period.

Microclimate measurements were made at a station installed at the step–pool unit. Net and solar radiation, air temperature and relative humidity, and wind speed were measured directly over the water surface upstream of the step. Instruments included a Micromet Systems net radiometer, Eppley pyranometer, a Campbell Scientific CS-500 temperature and humidity probe and a Met One anemometer. Instruments were scanned every second and averaged every 10 min by a Campbell Scientific CR21X data logger. Vapour pressure of the air was computed using the air temperature and relative humidity, while the vapour pressure at the water surface was computed as the saturation value corresponding to water temperature.

Bed temperature profiles within the step–pool unit were measured at 19 locations with copper–constantan thermocouples at depths of 5, 10 and 20 cm below the surface (Figure 1). Each set of thermocouples was fixed onto a wooden stake (approximately 1–2 cm^2 in cross-section) that was inserted to the required depth. At four of the thermocouple profiles (two above the step, two in the pool), water temperature was measured using thermocouples mounted 2 cm above the bed. Temperatures were recorded every 10 min using Campbell Scientific CR21X loggers connected to multiplexers. Thermocouple measurements should be accurate to within $\pm 0{\cdot}2\,^{\circ}C$ under most conditions.

Vertical hydraulic gradients during summer 2001 were measured using piezometers constructed of 1-cm inside diameter aluminium pipe that had been crimped and tapered at the lower end to allow driving. Holes were drilled through the bottom 5 cm, and the piezometers were driven to a depth of 30 cm below the bed surface at 12 locations (Figure 1). Unfortunately, we were unable to drive any of these piezometers into the pools, where substrate was dominated by cobbles. In summer 2003, we installed 14 piezometers constructed of 1-cm outside diameter plexiglass tubing, with holes drilled over the bottom 3 cm, including eight in pool locations and six in the riffle/step areas. These piezometers were installed to depths of 20–30 cm using an approach similar to that described by Baxter *et al.* (2003). Water levels inside the piezometers were measured using a 'dip-stick' with electrical contacts at the lower end, so that a buzzer sounded when the contacts reached the water surface. Water level measurements were accurate to within about ± 3 mm.

To conduct slug tests in the plexiglass piezometers, a syringe was connected by tygon tubing to the top of the piezometer tube and was used to draw water up the tube. After the water level stabilized in the piezometer, the tygon tube was disconnected and the time taken for the water to drop to a marked point was measured with

a stopwatch. Three or more successful trials were conducted at five piezometers within the downwelling zone. Hydraulic conductivity was computed using a two-point version of Hvorslev's (1951) method, as described by Baxter *et al.* (2003).

Streamflow was measured at a v-notch weir at the lower end of the study reach using a pressure transducer to record stage. Groundwater inflow along the study reach was estimated by assuming that streamflow was proportional to drainage area because the complex channel morphology precluded accurate measurement of streamflow, especially at the upper end of the reach.

Estimating the effect of forest harvesting

A paired-catchment approach was used to estimate the effects of forest harvesting on stream temperature (Hewlett, 1982). Regression relations were derived for the pre-logging period between daily minimum, mean and maximum stream temperatures at A Creek as a function of the corresponding values at the unlogged control, East Creek. Generalized least-squares regression was used to account for residual autocorrelation, using the implementation in the software package S-Plus. The fitted model was:

$$y_t = \beta_0 + \beta_1 x_t + \beta_2 \sin(2\pi j/T) + \beta_3 \cos(2\pi j/T) + \varepsilon_t \quad (1)$$

where y_t is the temperature at A Creek on day t, x_t is the temperature at the control, β_0, β_1, β_2 and β_3 are coefficients to be estimated by regression, j is day of the year ($j = 1$ on 1st January), $T = 365{\cdot}25$, the number of days in a year, and ε_t is an error term, modelled as an autoregressive process of order k:

$$\varepsilon_t = \rho_1 \varepsilon_{t-1} + \rho_2 \varepsilon_{t-2} + \cdots + \rho_k \varepsilon_{t-k} + u_t \quad (2)$$

where ρ_i is the autocorrelation between error terms at a lag of i days, ε_{t-i} is the error term i days before day t, and u_t is a random disturbance, assumed to be normally distributed with constant variance. The order k was determined by examining partial autocorrelation plots of the pre-logging residuals and retaining only the terms with statistically significant partial autocorrelation coefficients. The sine and cosine terms in Equation (1) account for seasonality in the residuals (Watson *et al.*, 2001).

The treatment effect on a given day in the post-harvesting period (T_e) was estimated as the difference between the observed post-logging temperatures at A Creek and values predicted from the pre-logging regression:

$$T_e = y_t - \hat{y}_t \quad (3)$$

where y_t and $\hat{y}_t$ are the observed and predicted temperatures on day t.

Estimating hyporheic exchange

Hyporheic exchange rates have been estimated in many previous studies by analysing tracer injection experiments (e.g., Harvey and Bencala, 1993; Story *et al.*, 2003). However, analysis of tracer breakthrough curves cannot distinguish between hyporheic exchange and transient storage in pools. During periods of low flow in these steep, headwater streams, the stream essentially becomes a series of pools linked by flow through riffles or over the step-forming elements, thus confounding interpretation of tracer breakthrough curves. In addition, we were restricted from conducting tracer injections due to concerns by managers of a fish hatchery downstream of the study reach. As an alternative, hyporheic water flux per unit stream length (F_{hyp}; $m^3\ s^{-1}\ m^{-1}$) was computed as

$$F_{hyp} = A_{inf} q_z / L_{s-p} \quad (4)$$

where A_{inf} is the area (m^2) over which infiltration into the bed occurred upstream of a step, q_z is the vertical flux of water infiltrating the stream bed ($m\ s^{-1}$), and L_{s-p} is the average spacing between step–pool units, each of which is assumed to represent a complete hyporheic flow path (m) (i.e., all the water that infiltrates upstream of a step re-emerges in the pool below the step).

Infiltration rates were estimated by two approaches. The first is based on Darcy's law:

$$q_z = K_{\text{sat}} \Delta h / \Delta z \tag{5}$$

where K_{sat} is the saturated hydraulic conductivity of the bed (m s^{-1}), determined from slug tests as described above, and $\Delta h/\Delta z$ is the absolute value of the mean vertical hydraulic gradient determined from piezometers in the area of downwelling. The vertical water flux was also estimated as

$$q_z = \phi v \tag{6}$$

where ϕ is the porosity of the bed material and v is the mean vertical velocity of pore water. Velocities of infiltrating water were estimated from bed temperatures for the period August 13 to 15, which was dominated by clear-sky conditions, low flow, and included the highest stream temperatures recorded during the 2001 study period. Cross-correlation functions were computed between the 5-cm bed temperature time series (for thermocouples located in downwelling areas, as inferred from the piezometers) and the stream water temperatures. Velocities were estimated as:

$$v = (0{\cdot}05 \text{ m})/\tau_{\max} \tag{7}$$

where $\tau_{\max}$ is the lag corresponding to the maximum cross-correlation (s), which was assumed to approximate the travel time from the stream bed to a depth of 5 cm.

Analysis of bed temperature patterns in relation to surface–subsurface interactions

Zones of upwelling, downwelling and neutral vertical exchange were identified based on the piezometer measurements (Figure 1), and were used to classify the hydrologic setting of each thermocouple profile. The mean, minimum and maximum temperatures over the study period were computed for each thermocouple. These were then analysed by a two-way ANOVA, with depth (5, 10 and 20 cm) and hydrologic setting (upwelling, downwelling, neutral) as fixed effects to assess the statistical significance of differences.

Heat budget estimates

Many previous studies have formulated stream heat budgets in relation to the longitudinal change in temperature of water as it flows through a stream reach (e.g., Brown, 1969; Sinokrot and Stefan, 1993; Webb and Zhang, 1997). Given the very low flows that dominated during the periods of high stream temperature and the influences of the pools, it is difficult to determine the travel time through a reach for A Creek. To address this problem, an alternative heat budget formulation is presented below, which expresses the heat budget in terms of changes in heat storage within a stream reach.

The heat and water budgets for a stream reach can be expressed as:

$$\begin{aligned}\rho c_{\text{p}} w_{\text{s}} L d_* \frac{d\langle T\rangle}{\text{d}t} = {} & \rho c_{\text{p}} F_{\text{us}} T_{\text{us}} + \rho c_{\text{p}} L F_{\text{gw}} T_{\text{gw}} + \rho c_{\text{p}} L F_{\text{hyp}} (T_{\text{hyp}} - \langle T\rangle) \\ & + w_{\text{s}} L (Q_* + Q_{\text{h}} + Q_{\text{e}} + Q_{\text{c}}) - \rho c_{\text{p}} F_{\text{ds}} T_{\text{ds}}\end{aligned} \tag{8}$$

and

$$F_{\text{ds}} = F_{\text{us}} + L F_{\text{gw}} \tag{9}$$

where ρ = water density (kg m^{-3}), c_{p} = specific heat of water (J kg^{-1} K^{-1}), w_{s} = mean surface width (m), L = reach length (m), d_* = mean depth (m), $\langle T\rangle$ = spatial mean water temperature within the reach (°C), F_{us} = streamflow at upstream end of the reach (m^3 s^{-1}), T_{us} = temperature at upstream boundary (°C), F_{gw} = groundwater inflow rate (m^3 s^{-1} m^{-1}), T_{gw} = groundwater temperature (°C), F_{hyp} = hyporheic exchange rate (m^3 s^{-1} m^{-1}), T_{hyp} = temperature of upwelling hyporheic flow (°C), Q_* = net radiation

(W m^{-2}), Q_h = sensible heat flux from the overlying air (W m^{-2}), Q_e = latent heat exchange (W m^{-2}), Q_c = bed heat conduction (W m^{-2}), F_{ds} = discharge at lower reach boundary (m^3 s^{-1}) and T_{ds} = temperature at downstream boundary (°C). The left-hand side of Equation (8) represents the rate of change of heat storage within the reach, and the terms on the right-hand side respectively represent heat inputs from upstream, heat inputs via groundwater inflow, heat transfer associated with hyporheic exchange, vertical energy exchange across the water surface and bed, and heat outputs to downstream reaches. Equation (8) does not include the sensible heat loss associated with the removal of water by evaporation or heat generation by friction as they were both found to be negligible for the study period. Energy exchange terms are considered positive if they represent an energy input.

Combining Equations (8) and (9) yields:

$$\frac{d\langle T\rangle}{dt} = \frac{F_{us}(T_{us} - T_{ds})}{w_s L d_*} + \frac{Q_* + Q_h + Q_e + Q_c + Q_{gw} + Q_{hyp}}{\rho c_p d_*} \tag{10}$$

where Q_{gw} and Q_{hyp} are energy fluxes associated with groundwater inflow and hyporheic exchange, respectively, given by:

$$Q_{gw} = \frac{\rho c_p F_{gw}(T_{gw} - T_{us})}{w_s} \tag{11}$$

and

$$Q_{hyp} = \frac{\rho c_p F_{hyp}(T_{hyp} - \langle T\rangle)}{w_s} \tag{12}$$

Net radiation was modelled by using the spatial distribution of gap fraction from the hemispherical photographs to compute direct and diffuse components of shortwave radiation and incoming longwave radiation (see Appendix for details). The latent heat flux was computed using the following form of the Penman-type equation presented by Webb and Zhang (1997):

$$Q_e = 285{\cdot}9(0{\cdot}132 + 0{\cdot}143u_a)(e_a - e_w) \tag{13}$$

where u_a is the wind speed measured at a height of about 1 m over the water surface (m s^{-1}), e_a and e_w are the vapour pressures of the air and water, respectively (kPa), and the constants account for the various unit conversions, physical constants such as the latent heat of vaporization, and empirical constants in the Penman equation. The sensible heat flux was computed as

$$Q_h = [\gamma(T_a - T_w)/(e_a - e_w)]Q_e \tag{14}$$

where γ is the psychrometric constant (kPa °C^{-1}).

Bed heat conduction was computed using Fourier's law:

$$Q_c = K_c(T_b - T_w)/(0{\cdot}05\ \text{m}) \tag{15}$$

where K_c is the thermal conductivity (W m^{-1} °C^{-1}), and T_b is the bed temperature measured at a depth of 0·05 m. We used an assumed thermal conductivity of $K_c = 2{\cdot}6$ W m^{-1} K^{-1}, based on the graphical relation of Lapham (1989) and assuming a porosity of 0·30, based on typical values for sands and gravels (Freeze and Cherry, 1979). A mean temperature gradient was computed based on the four thermocouples for which water temperature was measured 2 cm above the bed (two in upwelling and two in downwelling zones).

The temperature of upwelling hyporheic flow was assumed to equal the 5-cm bed temperature measured in the pools, where the piezometers indicated upwelling occurred. Groundwater temperature was assumed to equal the daily minimum stream temperature measured 10 m upstream of the cut block under a full canopy (12 °C). This value is somewhat higher than mean annual air temperature (9·2 °C), which is commonly used to approximate groundwater temperature. However, we feel the higher temperature is more appropriate, given

that lateral inflow is primarily via a shallow layer at the base of the soil profile, rather than from a deep aquifer.

RESULTS

Overview of the study period

Instrumentation was installed in early July, 2001. Generally dry and warm conditions dominated, with one major rainstorm (Figure 3). The warmest stream temperatures were recorded for August 13–15, during a period of cloudless-sky conditions and low flows.

Paired-catchment analysis of temperature response to harvesting

Results of the generalized least-squares analysis are summarized in Tables I and II. Minimum temperatures exhibited the greatest degree of residual autocorrelation in the pre-logging regression, significant to three lags, suggesting that it is most influenced by heat storage. Daily maximum temperatures increased up to 5 °C during summer, although the treatment effect varied substantially (Figure 4). The effect on minimum temperatures

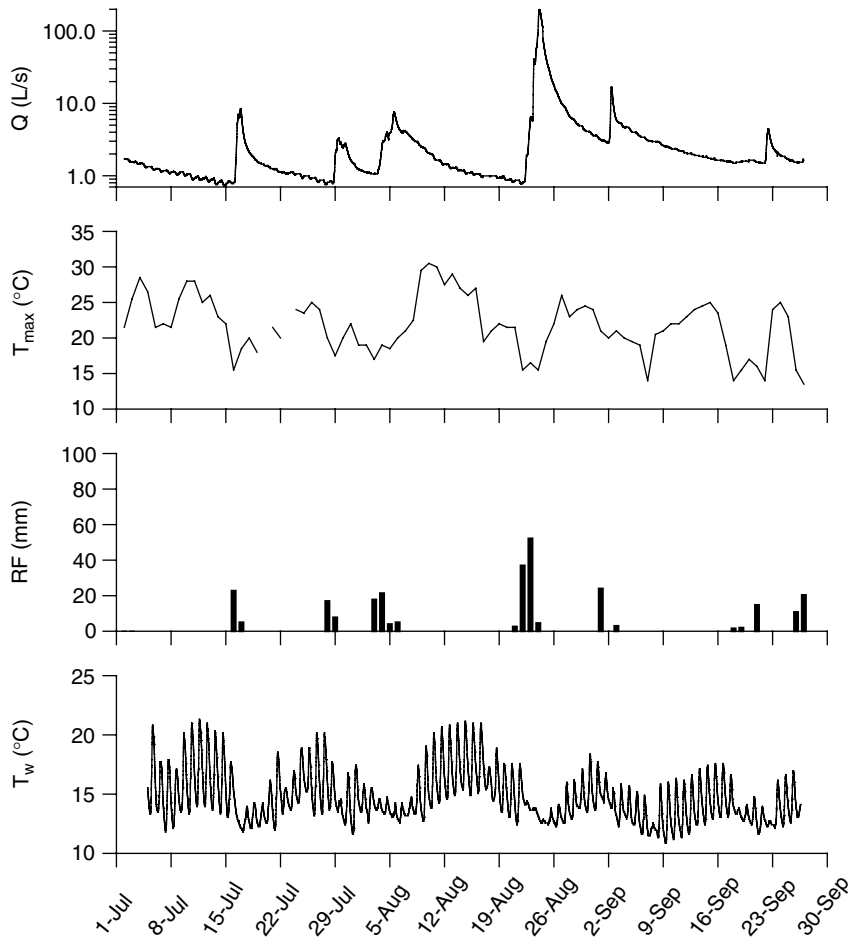

Figure 3. Weather and streamflow during the 2001 study period. From top to bottom: stream discharge; maximum daily air temperature; daily total rainfall; water temperature measured at 220 m

Table I. Results of generalized least squares regression analysis. The coefficients b_0 to b_3 are estimates of the parameters β_0 to β_3, with the significance levels (p values) shown in brackets, k is the order of the residual autocorrelation, s_e is the standard error of estimate, d.f. is the pre-logging degrees of freedom, and $\hat{\rho}_i$ is the estimated lag-i autocorrelation of the error terms

Temperature variable	d.f.	k	$\hat{\rho}_1$	$\hat{\rho}_2$	$\hat{\rho}_3$	b_0 (p value)	b_1 (p value)	b_2 (p value)	b_3 (p value)	s_e of residuals
Maximum	510	1	0·771	—	—	0·401 (0·115)	1·135 (<0·001)	0·218 (0·053)	−0·291 (0·023)	0·461
Mean	510	2	1·075	−0·235	—	0·769 (<0·001)	1·073 (<0·001)	0·024 (0·768)	−0·363 (<0·001)	0·338
Minimum	510	3	0·618	0·080	0·080	0·547 (<0·001)	1·083 (<0·001)	0·029 (0·706)	−0·182 (0·036)	0·303

Table II. Summary of mean temperatures and deviations from the fitted GLS regression relation for pre- and post-harvest periods

Temperature variable	Period	Mean	Magnitude of deviation from pre-logging regression		
			Max	Mean	Min
Daily maximum	Pre-logging	11·1	1·3	0·0	−1·6
	Post-logging	10·2	5·0	1·3	−1·0
Daily mean	Pre-logging	10·6	0·8	0·0	−1·3
	Post-logging	9·2	3·0	0·6	−1·0
Daily minimum	Pre-logging	10·2	1·0	0·0	−0·9
	Post-logging	8·4	2·8	0·2	−1·9

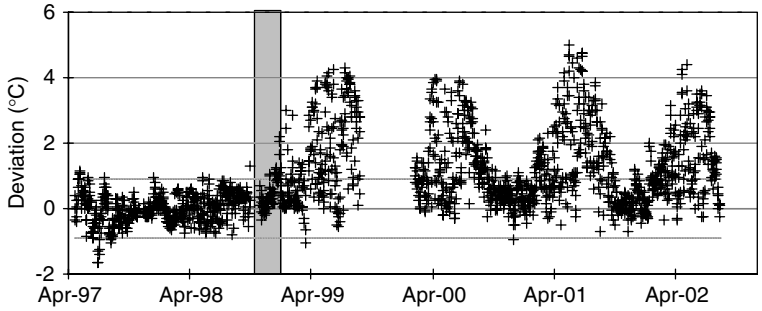

Figure 4. Time series of deviations from the pre-harvest regression between treatment and control streams for daily maximum stream temperature. The shaded area indicates the harvesting period. Horizontal lines indicating ±1·96 standard errors for the pre-logging regression are included to provide a visual reference

was relatively minor, with increases and decreases of about 1 °C in summer and winter, respectively. Daily mean temperatures increased up to 3 °C in summer.

Spatial and temporal variations in stream temperature

On warm days, temperatures increased steeply within the first 50 to 70 m below the upper end of the cut block, then at a lower rate to a distance of 300 m below the upper end of the cut block (25 m upstream of the lower end of the cut block) (Figure 5). Temperatures then decreased with distance through the lower 25 m

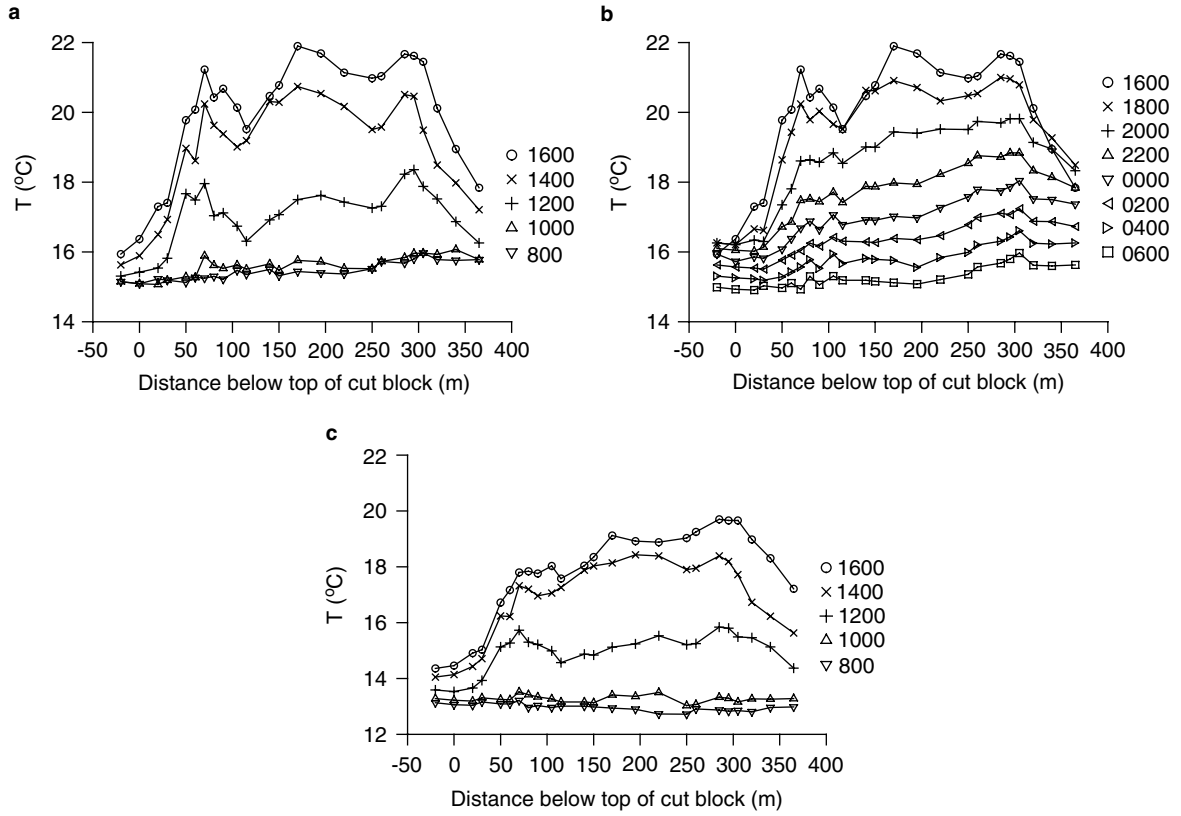

Figure 5. Longitudinal variations in stream temperature: (a) profiles at 2-h intervals during the warming phase on August 13; (b) profiles at 2-h intervals during the cooling phase of August 13–14; (c) profiles at 2-h intervals during the warming phase of August 8

of the cut block and an additional 50 m below the cut block. On August 13, temperatures decreased with distance downstream between 50–120 m and 170–250 m below the upper end of the cut block. The section from about 50 to 100 m has a steep relation between cumulative drainage area and distance, suggesting that it receives relatively concentrated lateral inflow (Figure 2). The section from 170 to 250 m also has a slightly steeper-than-average relation between cumulative drainage area and distance.

The sensitivity of maximum daily stream temperature to maximum daily air temperature (an index of energy input) and the logarithm of mean daily discharge varied along the reach (Table III). Loggers under the canopy both above and below the cut block ($x = -20$ m and 365 m) were apparently not sensitive to discharge variations, and had much lower sensitivity to air temperature compared to loggers in the clear-cut. The sensitivities to both air temperature and discharge increased rapidly with distance up to about 50 m into the clear-cut, then increased gradually up to about 300 m, consistent with the patterns in Figure 5. The residuals from the regressions exhibited strong order-one autocorrelation ($\hat{\rho}_1 > 0{\cdot}6$), suggesting that heat storage, probably in the bed and riparian zone, influenced the day-to-day stream temperature reponse.

The sensitivity to discharge can be seen in the comparison of warming profiles for August 8 and August 13 (Figure 5). Those days were similar in terms of weather conditions, with daily maximum air temperatures measured above the stream of 30·3 °C and 28·4 °C, respectively. However, discharge decreased from about 2·24 l s^{-1} on August 8 to 1·15 l s^{-1} on August 13. The higher flow on August 8 was associated with depressed temperatures throughout the cut block relative to those observed on August 13, especially at distances of about 50 to 100 m.

Table III. Results of ordinary least-squares regression analysis of daily maximum water temperature ($T_{w\,max}$) as a function of daily maximum air temperature ($T_{a\,max}$) and the logarithm of mean daily discharge (log Q). The fitted model is $T_{w\,max} = b_0 + b_1 T_{a\,max} + b_2 \log Q + e$. Results are shown only for a selection of locations, measured relative to the upper edge of the cut block

Location (m)	b_0	b_1	b_2	R^2_{adj}	s_e	n	$\hat{\rho}_1$
−20	9·94	0·168	n/s	0·54	0·68	80	0·67
0	8·31	0·194	−0.461	0·61	0·74	80	0·66
20	7·29	0·235	−0.641	0·66	0·81	80	0·67
50	2·55	0·344	−2.06	0·76	1·08	80	0·71
105	3·86	0·349	−1.68	0·82	0·88	80	0·63
220	2·68	0·389	−2.07	0·82	0·99	80	0·66
295	2·03	0·421	−2.24	0·83	1·03	80	0·64
365	9·59	0·261	n/s[1]	0·70	0·76	80	0·66

Note: n/s = not significant.

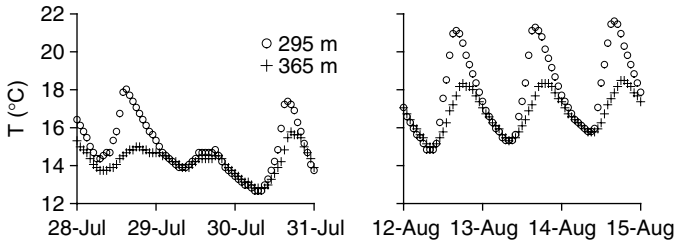

Figure 6. Temperature patterns at 295 m (within the cut block) and 365 m (downstream of the cut block)

The temperature changes between 295 m and 365 m below the upper end of the cut block were mainly evident in the maximum temperature on warm days (Figure 6). There was little change on cool days (e.g., Figure 6, July 29–30), and even on warm days, the daily minima were similar at both locations.

At the scale of the step–pool unit, stream temperature variations of up to about 2 °C were observed during warm spells, based on four thermocouples mounted 2 cm above the bed and a Tidbit logger located in the upstream pool (data not shown). Although two of the pool locations were cooler than the step locations, the third had almost identical temperatures to the step locations. This variability may relate to the existence of focused areas of upwelling water, which could create localized cool-water zones, especially for measurements taken near the bed. During cooler weather, differences amongst the five locations were less than 0·5 °C.

Piezometer measurements and bed temperature variations

The hydraulic head measurements made in 2001 and 2003 allowed us to identify downwelling, neutral and upwelling zones within the step–pool unit (Figure 1). Bed temperatures in downwelling zones tended to have greater diurnal ranges on warm days than in neutral and downwelling zones, although there was substantial lateral variability in bed temperatures within each hydrologic setting, up to about 2 to 4 °C (Figure 7). At all depths, maximum temperatures were greatest in downwelling zones, intermediate in neutral zones and lowest in the pools, with an average difference over the study period of about 2 °C between downwelling zones and pools (Figure 8). Minimum temperatures displayed the inverse pattern, being up to about 0·5 °C lower in downwelling areas than in pools. Mean temperatures over the study period tended to be slightly higher in downwelling zones, but the contrast was less than 0·5 °C for all depths. Two-way analysis of variance indicated that the effect of hydrologic setting was highly significant ($p < 0{\cdot}001$ for minimum,

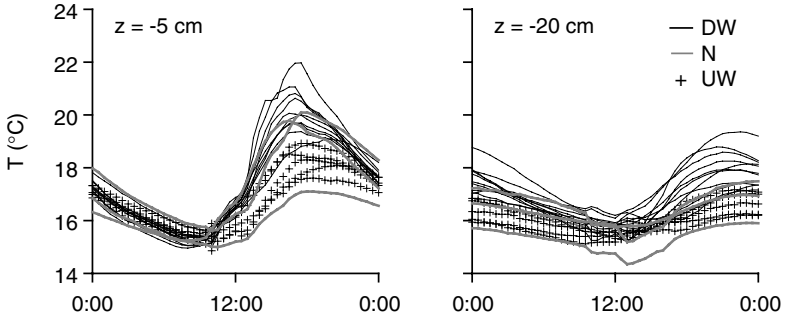

Figure 7. Bed temperatures on August 13, 2003 at 5 cm and 20 cm depth. UW = upwelling, N = neutral, DW = downwelling

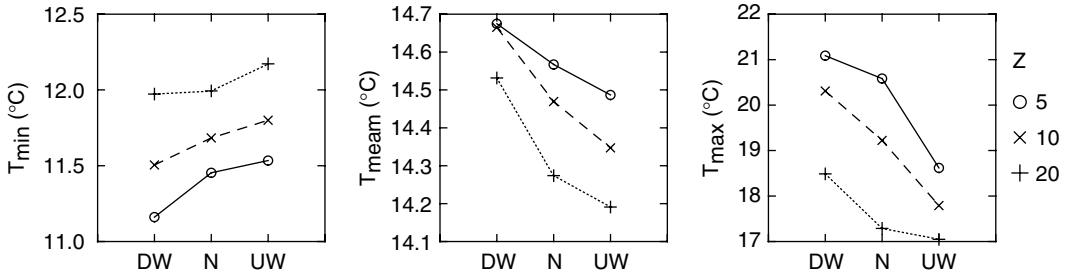

Figure 8. Spatial averages of minimum, mean and maximum bed temperatures recorded during the study period, grouped by hydrologic setting in the step–pool unit and by depth

mean and maximum temperatures). However, the significance levels must be interpreted cautiously, since the distributions of residuals were non-normal. Also, spatial correlation amongst profile locations would invalidate the assumption of independence.

The lags associated with the maximum cross-correlation between 5-cm bed temperatures and water temperature varied from 0 to 12 10-min intervals for the thermocouple profiles located in downwelling zones, with a median of 3·5 intervals ($n = 10$). For comparison, the lags associated with maximum cross-correlation had means of 8 ($n = 3$) and 12·5 intervals ($n = 4$) and medians of 10 and 12 intervals for the neutral and upwelling profiles, respectively. To convert the lags for the downwelling profiles into velocities, the lag value of 0 was arbitrarily changed to 0·25 (on the basis that it really lay somewhere between 0 and 0·5). The resulting velocities ranged from $6{\cdot}9 \times 10^{-6}$ m s^{-1} to $3{\cdot}3 \times 10^{-4}$ m s^{-1}, with a mean of $5{\cdot}5 \times 10^{-5}$ m s^{-1} (standard error $3{\cdot}1 \times 10^{-5}$ m s^{-1}) and median of $2{\cdot}4 \times 10^{-5}$ m s^{-1}. For an assumed porosity of 0·3, the mean vertical flux would be approximately $1{\cdot}7 \times 10^{-5}$ m s^{-1}.

Values of hydraulic conductivity from five piezometers tested in 2003 ranged from $6{\cdot}2 \times 10^{-5}$ m s^{-1} to $5{\cdot}2 \times 10^{-4}$ m s^{-1}, with harmonic, geometric and arithmetic means of $1{\cdot}3 \times 10^{-4}$, $1{\cdot}7 \times 10^{-4}$ and $2{\cdot}2 \times 10^{-4}$ m s^{-1}, respectively. These values are about an order of magnitude lower than what would be expected for the calibre of sediments viewed at the surface, which comprised a mixture of coarse sand, gravel and cobbles, compared to typical values for these sediments (Freeze and Cherry, 1979). This discrepancy suggests a downward fining of grain sizes, possibly due to infiltration of fines into the coarser matrix. Within the downwelling area, the vertical hydraulic gradients measured on August 14, 2001 ranged from about 0·03 to 0·21 m m^{-1}, with a mean of 0·09 m m^{-1}. The downward flux computed from Darcy's law is thus about $1{\cdot}5 \times 10^{-5}$ m s^{-1}, using the geometric mean conductivity. This value agrees well with the estimate based on temperature lags, although the agreement may be fortuitous, given the uncertainties inherent in both methods.

Heat budget estimates during a period of high stream temperature

We applied the heat budget approach to the segment of the stream between 70 m and 295 m to minimize the magnitude of the first term on the right-hand side of Equation (10). Channel geometry was estimated from measurements made on August 10, 2001 when 19 cross-sections were surveyed in the 225-m stream segment. The mean width and depth on that date were 1·82 m and 0·14 m (standard errors 0·05 m and 0·016 m), respectively, and the discharge was approximately 50% higher than on August 13. Stage and width measurements made on August 14 (when discharge was about 5% less than on August 13) indicated that pool depths had dropped by about 1·5 cm, while the width had decreased by 9 cm. Therefore, we used a mean depth of 0·125 m and a width of 1·73 m.

Solar radiation measured over the stream on August 13, 2001 approached that measured in the open at mid-day, but was truncated in the morning and afternoon by the surrounding slopes and riparian vegetation, and a shadow from a tree crossed over the pyranometer in late morning (Figure 9a). Modelled solar radiation was substantially reduced compared to the open site in the morning and afternoon, and was about 30% lower than the open site through the middle portion of the day, due to the shading effects of riparian vegetation, surrounding slopes and woody debris suspended over the stream.

The sensible and conductive heat exchanges were relatively minor terms during the day, on the order of 10% of net radiation, and tended to offset each other (Figure 9b). Groundwater inflow and latent heat exchange were also minor terms, and tended to cool the stream both night and day. The hyporheic heat flux exerted a small warming effect at night and a cooling effect during the day, particularly in late afternoon, when it reached about 25% of the magnitude of net radiation. The first term on the right-hand side of Equation (10), which represents the net heat input from upstream by advection, never exceeded 0·1 °C h^{-1} in absolute value, compared to observed rates of change up to over 1 °C h^{-1} (Figure 9c). The estimated values of $d\langle T\rangle/dt$

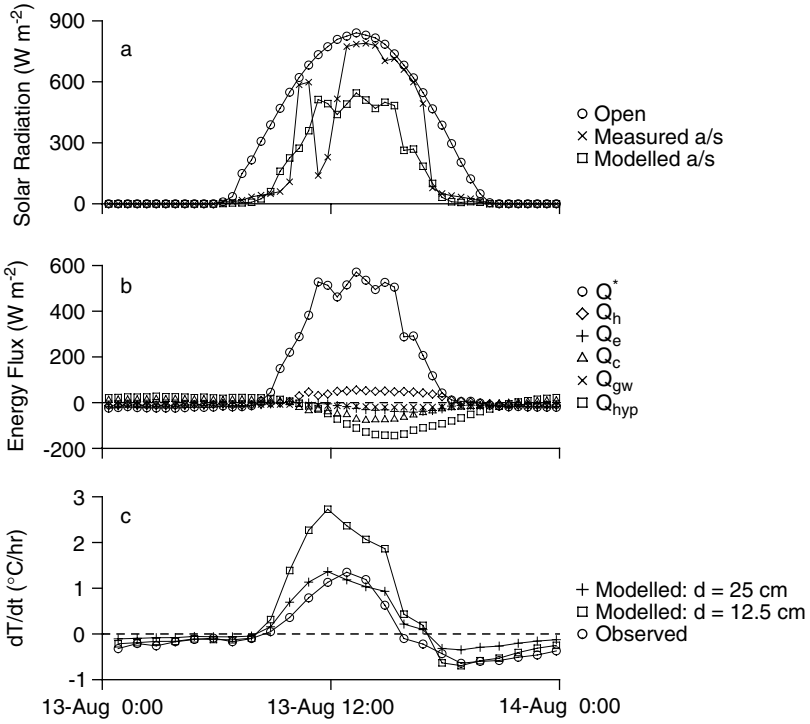

Figure 9. Heat budget results: (a) solar radiation (a/s = above stream); (b) heat budget components; (c) rate of change of temperature (d = mean depth used in model)

agreed reasonably with the observed values at night, but were up to three times too high during late morning (Figure 9c). Doubling the mean depth used in the calculation provided better agreement during the day, particularly in the early afternoon, but worsened the agreement at night (Figure 9c).

DISCUSSION

Effect of forest harvesting on stream temperature

The magnitude of the treatment effect at A Creek was smaller than has been documented for other streams impacted by clear-cut logging with no riparian buffer in the Pacific Northwest. For example, changes in summer maximum temperature of about 8 °C were observed at two streams in H. J. Andrews Research Forest in the western Cascades in Oregon (Johnson and Jones, 2000), while an increase of 13 °C was found at Needle Branch in the Oregon Coast Range (Harris, 1977). This difference may reflect the influence of the higher latitude and associated lower solar irradiance, as well as differences in groundwater influence, channel morphology and/or the magnitude of hyporheic exchange. For example, at Needle Branch, the catchment was broadcast-burned after harvest, and all wood was removed from the stream. It is possible that the removal of wood and loss of step–pool structures decreased hyporheic exchange and thus its cooling effect. Alternatively, burning in the riparian zone could have enhanced the receipt and absorption of solar radiation compared to the effect of clear-cutting without burning (Feller, 1981). Future experimental studies should include process measurements both before and after treatment in order to explain the observed magnitude of response. Without a physical basis for explaining the magnitude of post-harvest stream warming, it is difficult to generalize treatment effects to other cases.

The treatment effect exhibited substantial variability both within and among seasons, likely reflecting the variations in available energy, particularly incident solar radiation, on those time scales. As revealed by the regression analyses in Table III, clear-cutting apparently increased the stream's sensitivity to weather variations compared to an undisturbed location. Detailed analyses of treatment effects for a suite of streams subject to different riparian treatments will be presented in a future paper (Gomi *et al*., unpublished data).

Thermal heterogeneity

Thermal heterogeneity occurred at a range of spatial scales. At the broadest scale, the study reach consisted of three sections: an upper section, characterized by relatively high longitudinal gradients associated with rapid warming of the cooler water emerging from the forest; an intermediate zone, characterized by relatively low longitudinal gradients; and a cooling zone, including the lower part of the reach within the cut block and the full-canopy zone downstream of the cut block. The downstream cooling in the lower subreach was probably related to the decrease in solar radiation input caused by shading of the stream by the forest edge along the bottom of the cut block, coupled with cooling by groundwater inflow, hyporheic exchange and/or heat conduction into the bed, as was found by Story *et al*. (2003).

Embedded within these broader zones were two sections where temperatures decreased with downstream distance. These sections are associated with areas of relatively steep increases in drainage area. They are thus likely areas of concentrated lateral inflow, which could have a cooling effect both directly by diluting the warmer stream water, but also indirectly by maintaining cool bed temperatures, thus promoting heat loss by conduction and hyporheic exchange (Story *et al*., 2003). At the finest spatial scale, temperatures within the step–pool unit varied by up to 2 °C on warm days.

We did not systematically sample for lateral heterogeneity caused by differential shading of the stream surface, as has been documented by Clark *et al*. (1999). Therefore, such variability could have contributed to the observed longitudinal variability.

The documented thermal heterogeneity may be ecologically important. Depending on their mobility, some organisms may be able to take advantage of thermal variations to minimize exposure to high temperatures.

Thermal heterogeneity may also be important in relation to monitoring. A single temperature logger located at the lower end of a cut block will not provide an accurate measure of conditions throughout the impacted reach. In the case of A Creek, where downstream cooling began within the cut block, a logger at the lower end of the cut block would have underestimated maximum temperatures within the block by up to 2 °C. Loggers are often placed in pools to minimize the possibility of dewatering, particularly at remote sites that are not visited frequently. Variability in pool temperatures of up to 2 °C was observed on warm days, introducing another potential source of sampling variation that needs to be considered in designing monitoring programmes.

Bed temperature patterns

Bed temperatures exhibited a systematic variation at the scale of the step–pool unit, linked to the occurrence of downwelling, neutral and upwelling flow. Bed temperatures in areas of downwelling flow tended to track stream temperature more closely, with higher maxima and greater diurnal variations. Logging-related impacts on benthic temperatures may, therefore, be greatest in areas of downwelling flow. The observed bed temperature patterns represent a structuring of the benthic environment on small spatial scales, which may be significant in relation to rates of growth and development of benthic organisms. Further study should focus on stream–subsurface exchange in complex headwater streams and its relation to temperature patterns.

Heat budget results

The estimated energy fluxes suggest that the sensible and latent heat exchanges and bed heat conduction are secondary terms relative to net radiation, particularly during the daytime, when their net effect is small. This finding is consistent with Brown's (1969) finding in small Oregon streams, where net radiation dominated during daytime. While the hyporheic heat flux was also a secondary term, it accounted for up to 25% of net radiation during the period of the day with the greatest warming rate, and thus was not negligible.

There were significant errors in closing the heat budget; the modelled rate of temperature change was up to three times greater than observed during daytime. There are three possible causes of this error: (1) the net radiation input was overestimated; (2) the magnitudes of the cooling fluxes were underestimated; and (3) the water depth was underestimated. It is possible that stream shading was underestimated due to inadequate sampling, especially since our hemispherical photographs were taken near the centre of the stream and could have been biased. However, this is unlikely to be the sole explanation. The stream has shallow banks and is dominantly southwesterly in aspect. Hence, in the afternoon, the sun would have shone directly onto the stream, with relatively small opportunity for shading by the banks or riparian vegetation, which was dominantly low shrubs.

It is possible that one or more of the cooling fluxes could have been underestimated. Of these, groundwater is the least likely to have an effect. Increasing the rate of groundwater inflow ten times still resulted in overestimation of daytime heating, but also produced excessive nighttime cooling (results not shown). Evaporation could have been underestimated, especially since the Penman equation may not be applicable to this small stream with little fetch. However, during the daytime, the Bowen ratio was less than -1, indicating that an increase in evaporation would be more than offset by an increase in sensible heat exchange (assuming similarity of heat and vapour transport). Bed heat conduction could have been underestimated, both because we only sampled bed temperature gradients at one site, and also because the assumed thermal conductivity could be in error. In addition, our equal weighting of bed temperature gradients between upwelling and downwelling zones may have been incorrect. The hyporheic exchange could also have been underestimated, particularly because we only sampled one step–pool unit, and our calculation only accounts for the component of hyporheic exchange associated with downwelling into steps. A number of studies have shown that significant hyporheic exchange also occurs by lateral movement out of the stream at the heads of steps and riffles (e.g., Harvey and Bencala, 1993; Kasahara and Wondzell, 2003). Furthermore, our estimated vertical flux rate is likely subject to considerable uncertainty.

Although it is possible that we underestimated the mean depth, the standard error was only 11% of the mean, suggesting that an error greater than about 25% of the mean would be highly unlikely. Thus, we feel that error in the estimated mean depth can only explain part of the error in closing the heat budget.

The heat budget equation derived for use in this study has the advantage that it does not require knowledge of stream velocity, and thus may be more easily applicable to conditions of very low flow, when velocities are low and the stream becomes a series of pools linked by short riffles and steps. However, its application requires detailed sampling of channel geometry, given that $d\langle T\rangle/\mathrm{d}t$ is inversely proportional to mean depth. A fundamental issue in estimating heat budgets for small streams is the need for detailed sampling of canopy characteristics because of the complex shading patterns resulting from the surrounding topography, riparian vegetation and logs suspended above the stream.

CONCLUSIONS

The paired-catchment analysis revealed that daily maximum temperatures increased up to about 5 °C after logging, and were positively associated with daily maximum air temperature and negatively with discharge. Although there was a general trend to increasing daily maximum temperature with downstream distance through the cut block, daily maximum temperature decreased with downstream distance in two segments over distances of tens of metres, in locations where the topography indicated relatively concentrated lateral inflow. Bed temperatures tended to be greater and have higher ranges in areas of downwelling flow into the bed.

Net radiation dominated the heat budget during the daytime. Heat exchange associated with hyporheic flow paths was a cooling effect during daytime, with a magnitude up to approximately 25% that of net radiation during the period of maximum daytime warming. Errors in closing the heat budget could have arisen through overestimation of solar radiation reaching the stream surface, underestimation of cooling fluxes, particularly bed heat conduction and hyporheic exchange, and underestimation of stream depth. Further research should focus on characterizing hyporheic flow paths associated with these step–pool structures and their influence on stream and bed thermal regimes.

APPENDIX: DETAILS OF RADIATION MODEL

Although net radiation was measured directly over the stream surface, the site was variably shaded by the surrounding slopes and riparian vegetation. Furthermore, shade conditions varied substantially along the stream. Therefore, reach-averaged estimates of net radiation were developed for one day characterized by clear-sky conditions (August 13, 2001). The model can be expressed as

$$Q_* = (1-\alpha)[D(t)g(t) + S(t)f_\mathrm{v}] + [f_\mathrm{v}\varepsilon_\mathrm{a} + (1-f_\mathrm{v})\varepsilon_\mathrm{f}]\sigma(T_\mathrm{a} + 273{\cdot}2)^4 - \varepsilon_\mathrm{w}\sigma(T_\mathrm{w} + 273{\cdot}2)^4 \qquad \text{(A1)}$$

where α is the albedo of the stream, $D(t)$ is the direct component of incident solar radiation at time t (W m^{-2}), $g(t)$ is the canopy gap fraction at the sun's sky position at time t, $S(t)$ is the diffuse component of incident solar radiation at time t (W m^{-2}), f_v is the sky view factor, ε_a, ε_f and ε_w are the emissivities of the atmosphere, foliage and water, σ is the Stefan–Boltzmann constant ($5{\cdot}67 \times 10^8$ W m^{-2} K^{-4}), T_a and T_w are the temperatures of air and water, respectively (°C). The atmospheric emissivity was computed using the Idso (1981) equation for clear-sky conditions. The emissivity and albedo of water were assumed to be 0·95 and 0·05, respectively.

The distribution of gap fraction as a function of zenith angle (θ) and azimuth (a_s), $g_*(\theta, a_\mathrm{s})$, was derived by analysing the hemispherical photographs with the Gap Light Analyser software (Frazer *et al.*, 1999), using 5° increments for both zenith and azimuth angles. The canopy gap function, $g(t)$, was derived from $g_*(\theta, a_\mathrm{s})$ by computing the solar zenith and azimuth angles as a function of t. The view factor was computed as

$$f_\mathrm{v} = \frac{1}{\pi}\int_0^{2\pi}\int_0^{\pi/2} g_*(\theta, a_\mathrm{s})\cos\theta\sin\theta\ \mathrm{d}\theta\ \mathrm{d}a_\mathrm{s} \qquad \text{(A2)}$$

where θ is the solar zenith angle (vertical = 0), a_s is the azimuth angle, and $g_*(\theta, a_s)$ is the gap fraction at sky position θ, a_s. The double integral was approximated by summations using an interval of 5° for both zenith and azimuth angles.

Solar radiation measurements made in a clear-cut about 2 km from A Creek during 2003 were used as input to the radiation model. Two Kipp and Zonen CM-6B pyranometers were scanned every second and averaged every 10 min using a Campbell Scientific CR10X logger. One pyranometer was fitted with a shadow band to block direct insolation and thus measure diffuse insolation. Direct insolation was computed as the difference between the total and diffuse components. Fortuitously, August 13, 2003 was cloud-free, so those data should be a reasonable proxy for incident solar radiation for August 13, 2001.

ACKNOWLEDGEMENTS

Michael Feller provided the discharge data. Matthew Gellis, Dion Whyte, Anthony Story, Arelia Werner and Xavier Pinto helped with field work and data preparation. Funding was provided by operating grants to RDM from Forest Renewal British Columbia (FRBC), the Forestry Investment Initiative (FII) and Natural Sciences and Engineering Research Council. PS, TG and AD were supported by funding through grants from FRBC and FII. This project is part of a broader FRBC- and FII-funded project titled 'Ecology and management of riparian–stream ecosystems: a large scale experiment using alternative streamside management techniques' (P.I. John Richardson). Anthony Story provided constructive comments on an earlier draft.

REFERENCES

Baxter C, Hauer FR, Woessner WW. 2003. Measuring groundwater–stream water exchange: new techniques for installing minipiezometers and estimating hydraulic conductivity. *Transactions of the American Fisheries Society* **132**: 493–502.

Beschta RL, Bilby RE, Brown GW, Holtby LB, Hofstra TD. 1987. Stream temperature and aquatic habitat: fisheries and forestry interactions. In *Streamside Management: Forestry and Fishery Interactions*, Salo EO, Cundy TW (eds). University of Washington, Institute of Forest Resources: Contribution No. 57, pp. 191–232.

Bilby RE. 1984. Characteristics and frequency of cool-water areas in a western Washington stream. *Journal of Freshwater Ecology* **2**: 593–602.

Brown GW. 1969. Predicting temperatures of small streams. *Water Resources Research* **5**: 68–75.

Brown GW, Krygier JT. 1970. Effects of clear-cutting on stream temperature. *Water Resources Research* **6**: 1133–1139.

Clark E, Webb BW, Ladle M. 1999. Microthermal gradients and ecological implications in Dorset rivers. *Hydrological Processes* **13**: 423–438.

Ebersole JL, Liss WJ, Frissel CA. 2003. Cold water patches in warm streams: physicochemical characteristics and the influence of shading. *Journal of the American Water Resources Association* **39**: 355–368.

Feller MC. 1981. Effects of clearcutting and slashburning on stream temperature in southwestern British Columbia. *Water Resources Bulletin* **17**: 863–867.

Frazer GW, Canham CD, Lertzman KP. 1999. Gap Light Analyser (GLA), Version 2·0: Imaging software to extract canopy structure and gap light transmission indices from true-colour fisheye photographs. User's Manual and Program Documentation. Simon Fraser University, Burnaby, B.C. and the Institute of Ecosystem Studies, Millbrook, NY.

Freeze RA, Cherry JA. 1979. *Groundwater*. Prentice-Hall: Englewood Cliffs, NJ.

Harris DD. 1977. *Hydrologic changes after logging in two small Oregon coastal watersheds*. Geological Survey Water-Supply Paper 2037. US Geological Survey, Washington, 31 pp.

Harvey JW, Bencala KE. 1993. The effect of streambed topography on surface–subsurface water exchange in mountain catchments. *Water Resources Research* **29**: 89–98.

Hewlett JD. 1982. *Forests and floods in light of recent investigation*. Canadian Hydrology Symposium 82 (June 14–18, 1982, Fredericton, New Brunswick). Associate Committee on Hydrology, Ottawa, pp. 543–559.

Hewlett JD, Fortson JC. 1982. Stream temperature under an inadequate buffer strip in the southeast piedmont. *Water Resources Bulletin* **18**: 983–988.

Hutchinson DG, Moore RD. 2000. Throughflow variability on a forested slope underlain by compacted glacial till. *Hydrological Processes* **14**: 1751–1766.

Hvorslev MJ. 1951. *Time lag and soil permeability in ground-water observations*. Bulletin No. 36, Waterways Experimental Station Corps of Engineers, US Army, Vicksburg, MI, pp. 1–50.

Idso SB. 1981. A set of equations for full-spectrum and 8–14 μm and 10·5–12·5 μm thermal radiation from cloudless skies. *Water Resources Research* **17**: 295–304.

Johnson SL, Jones JA. 2000. Stream temperature responses to forest harvest and debris flows in western Cascades, Oregon. *Canadian Journal of Fisheries and Aquatic Science* **57**(Suppl. 2): 30–39.

Kasahara T, Wondzell SM. 2003. Geomorphic controls on hyporheic exchange flow in mountain streams. *Water Resources Research* **39**(1): 1005.
Kiffney PM, Richardson JS, Feller MC. 2000. Fluvial and epilithic organic matter dynamics in headwater streams of southwestern British Columbia, Canada. *Archiv fur Hydrobiologie* **149**: 109–129.
Lapham WW. 1989. *Use of temperature profiles beneath streams to determine rates of vertical ground-water flow and vertical hydraulic conductivity*. US Geological Survey Water-Supply Paper 2337, 35 pp.
Macdonald JS, MacIsaac EA, Herunter HE. 2003. The effect of variable-retention riparian buffers on water temperatures in small headwater streams in sub-boreal forest ecosystems of British Columbia. *Canadian Journal of Forestry Research* **33**: 1371–1382.
Malard F, Mangin A, Uehlinger U, Ward JV. 2001. Thermal heterogeneity in the hyporheic zone of a glacial floodplain. *Canadian Journal of Fisheries and Aquatic Science* **58**: 1319–1335.
Malcolm IA, Soulsby C, Youngson AF. 2002. Thermal regime in the hyporheic zone of two contrasting salmonid spawning streams: ecological and hydrological implications. *Fisheries Management and Ecology* **9**: 1–10.
Ringler NH, Hall JD. 1975. Effects of logging on water temperature and dissolved oxygen in spawning beds. *Transactions of the American Fisheries Society* **104**: 111–121.
Shepherd BG, Hartman GF, Wilson WJ. 1986. Relationships between stream and intragravel temperatures in coastal drainages, and some implications for fisheries workers. *Canadian Journal of Fisheries and Aquatic Science* **43**: 1818–1822.
Sinokrot BA, Stefan HG. 1993. Stream temperature dynamics: measurements and modeling. *Water Resources Research* **29**: 2299–2312.
Story AC, Moore RD, Macdonald JS. 2003. Stream temperatures in two shaded reaches below cut blocks and logging roads: downstream cooling linked to subsurface hydrology. *Canadian Journal of Forest Research* **33**: 1383–1396.
Titcomb JW. 1926. Forests in relation to fresh water fishes. *Transactions of the American Fisheries Society* **56**: 122–129.
Watson F, Vertessy R, McMahon T, Rhodes B, Watson I. 2001. Improved methods to assess water yield changes from paired-catchment studies: application to the Maroondah catchments. *Forest Ecology and Management* **143**: 189–204.
Webb BW, Zhang Y. 1997. Spatial and temporal variability in the components of the river heat budget. *Hydrological Processes* **11**: 79–101.
Winfield N. 2002. *The role of wood in headwater channels and short-term channel responses to harvesting of second growth riparian forests in southwestern British Columbia*. Unpublished MSc thesis, The University of British Columbia, Vancouver.

